ACS APPLIED MATERIALS & INTERFACES

www.acsami.org

Research Article

Ultrathin Nanofibrous Membranes Containing Insulating Microbeads for Highly Sensitive Flexible Pressure Sensors

Taiyu Jin, Yan Pan, Guk-Jin Jeon, Hye-In Yeom, Shuye Zhang, Kyung-Wook Paik, and Sang-Hee Ko Park*

Cite This: https://dx.doi.org/10.1021/acsami.0c00448

Read Online

ACCESS | Metrics & More | Article Recommendations | Supporting Information

ABSTRACT: Highly sensitive and flexible pressure sensors were developed based on dielectric membranes composed of insulating microbeads contained within polyvinylidene fluoride (PVDF) nanofibers. The membrane is fabricated using a simple electrospinning process. The presence of the microbeads enhances porosity, which in turn enhances the sensitivity (1.12 kPa^{-1} for the range of 0−1 kPa) of the membrane when used as a pressure sensor. The microbeads are fixed in position and uniformly distributed throughout the nanofibers, resulting in a wide dynamic range (up to 40 kPa) without any sensitivity loss. The fluffy and nonsticky PVDF nanofiber features low hysteresis and ultrafast response times (~10 ms). The sensor has also demonstrated reliable pressure detection over 10 000 loading cycles and 250 bending cycles at a 13 mm bending radius. These pressure sensors were successfully applied to detect heart rate and respiratory signals, and an array of sensors was fabricated and used to recognize spatial pressure distribution. The sensors described herein are ultrathin and ultralight, with a total thickness of less than 100 μm, including the electrodes. All of the materials comprising the sensors are flexible, making them suitable for on-body applications such as tactile sensors, electronic skins, and wearable healthcare devices.

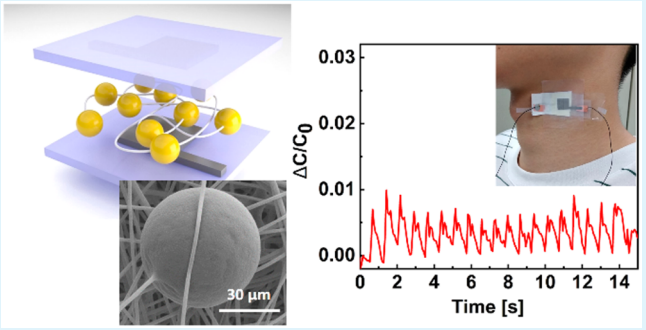

KEYWORDS: *wearable device, capacitive sensor, pressure sensor, microbead, nanofiber, electrospinning*

1. INTRODUCTION

Recently, wearable devices have attracted a lot of attention due to the increasing hand-held mobile device market, the urgent need for 24-h accessible smart devices, and the high application potential of the Internet of Things.[1,2] Pressure is a ubiquitous physical phenomenon produced by countless activities. Pressure represents the most basic sensory input from the environment, and numerous studies have aimed to develop pressure sensors for wearable devices.[3−5] Many types of pressure sensors convert mechanical movement to an electrical signal, including piezoresistive, capacitive, piezoelectric, and triboelectric sensors.[6−17] Most conventional pressure sensors are capacitive, due to the lower probability of mechanical failure and higher stability under practical working conditions. Capacitive pressure sensors feature a deformable dielectric that creates a large change in capacitance in response to a change in pressure.[18−21] Accordingly, many dielectric materials with high pressure sensitivity have been employed to create highly sensitive and flexible pressure sensors. For example, a stretchable tactile sensor was fabricated using a stretchable elastomer and electrodes.[22] The introduction of porous structures into the dielectric material can further enhance pressure-sensing capabilities. Kwon et al. obtained an Ecoflex sponge using a sugar cube template and Parameswaran et al. reported a polydimethylsiloxane (PDMS) sponge fabricated using yeast as a leavening agent.[23,24] Micropatterning of the elastomer into rough surfaces,[25−30] such as pyramids[18] and pillars,[31] as well as molding the elastomer from natural materials like silk[32] or leaves,[33,34] can improve sensor performance. Both methods increase the dielectric volume by introducing air gaps between the electrodes, which in turn reduces the Young's modulus of the dielectric layer and maximizes the capacitance change induced by a change in load. The smaller Young's modulus also allows a large amount of air to be squeezed out with less pressure. This results in a higher sensitivity by reducing the air component of the capacitor. We have summarized the studies reported previously, and compared the sensitivity in Table 1. The main method to achieve high sensitivity in these studies is to use elastic materials. By using micropatterning technology, it is very easy to control the number and size of microstructures, which

Received: January 9, 2020
Accepted: February 26, 2020
Published: February 26, 2020

Table 1. Comparative Methods of Fabricating Capacitive Pressure Sensors

method	material	sensitivity	pressure range	ref
pyramid shape	PDMS	0.55 kPa^{-1}	0–7 kPa	18
solid elastomer	Ecoflex + CNT	0.034 kPa^{-1}	0–25 kPa	22
sugar sponge	Ecoflex	0.601 kPa^{-1}	0–130 kPa	23
yeast sponge	PDMS	0.759 kPa^{-1}	0–40 kPa	24
SU8-spacer	PDMS	0.0655 kPa^{-1}	0–30 kPa	25
buckled surface	PDMS	3.8 kPa^{-1}	0–5 kPa	29
pillar shape	PDMS	0.42 kPa^{-1}	0–25 kPa	31
silk molding	PDMS	1.8 kPa^{-1}	0–1200 Pa	32
leaf molding	PDMS	0.815 kPa^{-1}	0–500 kPa	33

greatly improves the air gaps and reduces the overall Young's modulus. But this method requires additional microtemplates which adds one more process to prepare, and is not suitable for large-area fabrication either.

Pressure sensors fabricated using micropatterned elastomers are more flexible than silicon-based sensors. However, they are still too thick and costly for most wearable device applications.[23,35,36] Therefore, a flexible and sensitive pressure sensor that is both cost-effective and simple to fabricate remains highly desirable.[34]

Electrospinning is a simple and mature technology that can be used to make flexible, microstructured nanofibrous membranes.[37] Surface porosity, pore size, fiber thickness, and membrane thickness can be adjusted by controlling the electrospinning conditions. Over the past several decades, polyvinylidene fluoride (PVDF) has been widely used as a nanofiber material because of its flexibility, inherent biocompatibility, and low cost. Porous PVDF nanofiber webs have been used as high-performance electrolyte binders or separator films in batteries because of their large specific surface area.[38] PVDF nanofibers have also been used in pressure sensors, as both the substrate and the pressure-sensitive material.[39−42] These studies have shown that flexible, thin, nanofibrous PVDF membranes are suitable for a wide variety of applications.

This work describes an ultrathin, flexible capacitive pressure sensor based on electrospun PVDF nanofibers incorporating insulating microbeads. Nanofibers with conductive solder balls have been used to create anisotropic conductive films for ultrafine-pitch chip-on-glass interconnections.[43] Here, insulating microbeads were introduced into a PVDF solution prior to electrospinning, which resulted in a porous, nanofibrous membrane. In this study, we have used poly(methyl methacrylate) (PMMA) as the bead material, since it is a relatively soft polymer. We believe that using highly elastic materials will improve the sensing performance. The enhanced porosity of the membrane allowed for more significant mechanical deformation in response to changes in pressure. The microbeads were tightly anchored to the nanofibers, preventing microbead movement and aggregation. As a result, the nanofibrous membrane could be made exceptionally thin, which greatly shortened the preparation time and enhanced membrane stability over repeated endurance tests.

The pressure-sensing capability of our sensors was measured using a custom system that monitors changes in capacitance as a function of applied load. Sensitivity of up to 1.12 kPa^{-1} was observed over a range of 0–1 kPa. Pressure up to 40 kPa was measured without any appreciable loss in sensitivity. These

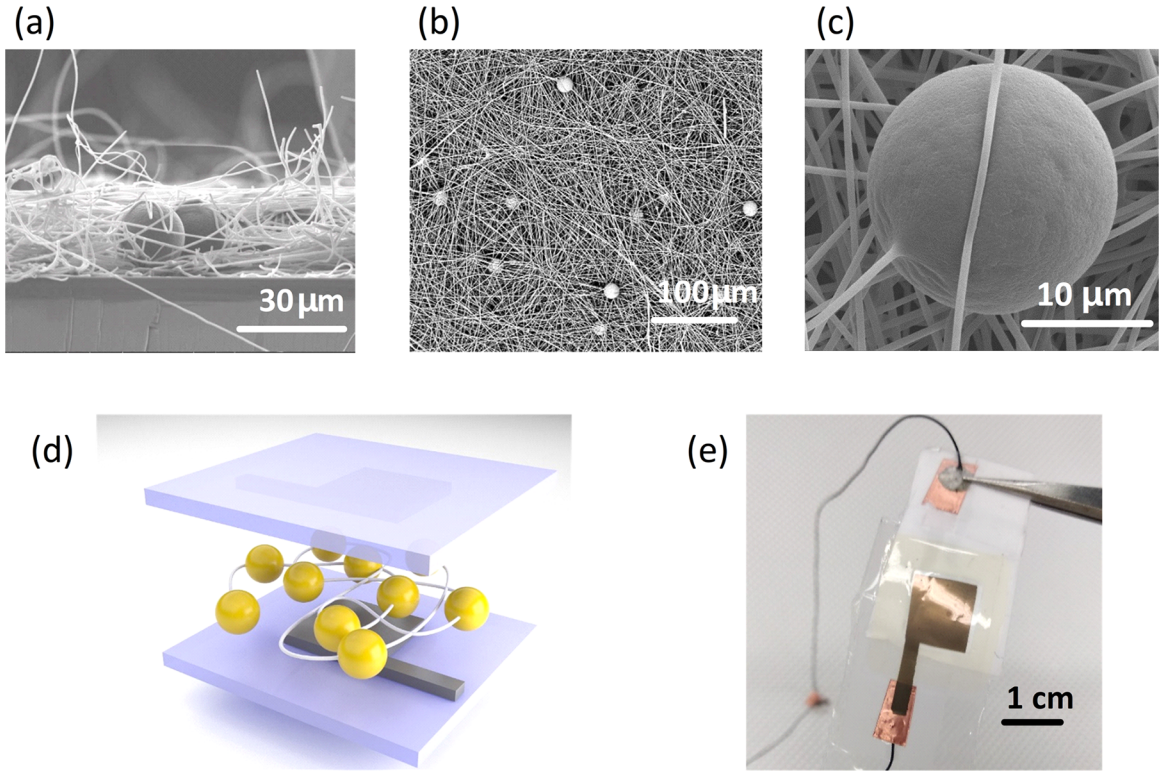

Figure 1. Schematic illustration of a flexible nanofiber/microbead pressure sensor. a) Scanning electron microscopy (SEM) cross section of a nanofibrous membrane. b) SEM micrograph of the nanofibrous membrane surface. c) SEM micrograph shows a microbead anchored by a nanofiber. d) Schematic diagram of the capacitive sensor architecture. e) Photograph of a nanofiber/microbead pressure sensor.

https://dx.doi.org/10.1021/acsami.0c00448
ACS Appl. Mater. Interfaces XXXX, XXX, XXX−XXX

sensors also exhibited low hysteresis, ultrafast response times (<10 ms), stability over 10,000 pressure cycles, and durability over 250 bending cycles. Furthermore, our sensors were applied as wearable heart rate (HR) and respiratory health monitors. Finally, a 5 × 5 sensor array was fabricated to demonstrate measurements of spatial pressure distribution.

2. RESULTS AND DISCUSSION

Variable thickness nanofibrous membranes were used as pressure-sensitive dielectric layers in capacitive pressure sensors. PVDF nanofibers alone are intrinsically nonelastic. Pure nanofibrous membrane sensors made from densely stacked PVDF nanofibers without any spacer materials usually exhibit low sensitivity and poor durability.[44] In addition, the diameter of a single nanofiber is on the nanometer scale, which limits the pressure response and requires long electrospinning times.

Large polymer beads have been added to nanofibers to increase the porosity of nanofiber membranes. These hybrid nanofibrous membranes have larger pores and a broader pore size distribution than pure nanofibrous membranes.[45,46] Hybrid nanofiber membranes incorporating microbeads and fabricated via electrospinning were expected to show huge mechanical deformation in response to an applied load. Figure 1a,b shows scanning electron microscopy (SEM) images of the surface and cross section of a nanofibrous membrane. The diameters of a single nanofiber and microbead were 300 nm and 20 μm, respectively.

This approach simplifies sample preparation and reduces fabrication time. The presence of microbeads increases membrane porosity and allows for the creation of high-performance dielectrics that can be tuned by controlling the air gap ratio. Although the thickness of the nanofiber stack is comparable to the diameter of a single bead, the beads are homogeneously distributed throughout the membrane. The thin nanofibrous membrane greatly enhances flexibility. In addition, since the microbeads are surrounded by PVDF nanofibers, they are fixed and cannot move freely within the membrane (Figure 1c). This stable membrane structure ensures high durability of the membrane. Figure 1d shows a schematic of our flexible, capacitive pressure sensor based on a metal-dielectric-metal sandwich layout. A 10-μm thin film of PVDF was cast by bar-coating and serves as a flexible substrate. Subsequently, a conductive electrode was applied, made by spray coating silver nanowires (AgNWs) on top of the PVDF film using a square screen mask for patterning. The sprayed silver wires were in contact with each other, forming a microweb structure. Then the AgNWs/PVDF film was annealed at the melting point of the PVDF, so that the melted PVDF will penetrate into the AgNWs microweb and the AgNWs will be completely embedded and protected in the PVDF film after cooling. In this way, the electrode maintains its conductivity even during the bending. The conductivity of the electrode was measured by four-point probe system and the sheet resistance is around 800 to ∼1100 mΩ/sq when the thickness of the AgNWs layer is around 500 nm.

A dilute PVDF solution containing a measured weight of microbeads was stirred vigorously to form a homogeneous dispersion. The well-mixed solution was then added to a syringe for electrospinning. During electrospinning, the application of a high electric field between a syringe containing a polymer solution and a grounded collector generates charges in the polymer. When the charge reaches a certain threshold, a stream of polymer solution bursts from the tip of the syringe, or nozzle, and is collected on a grounded collector plate, resulting in a nanofibrous membrane. Before electrospinning the PVDF/microbead mixture, the above AgNW/PVDF electrode was peeled from its substrate and attached to the surface of the collector, so that the nanofibrous hybrid membrane would be formed directly on the electrode surface.

Finally, to fabricate a capacitive sensor, upper and lower AgNW electrodes were placed face-to-face, separated by the hybrid nanofibrous membrane as shown in Figure 1d. Figure 1e shows a photograph of a completed pressure sensor. AgNW electrodes (1 cm × 1 cm) were patterned onto both the upper and lower PVDF films. A resin layer featuring a contact hole was formed on the upper electrode, which was laminated onto the nanofibers on the lower electrode. Square-shaped electrodes were aligned with the resin contact hole so that the effective sensor was at the overlapping region between the two conductive electrodes. Both the upper and lower sides of the nanofiber layer were covered with PVDF films, and PVDF itself is a hydrophobic material. These two factors kept the water outside from wetting the nanofibers through the film directly from the surface. Besides, the side of the sensor was sealed with resin during lamination process. Therefore, moisture or sweat would not affect the device in practical applications.[47] In addition, since the electrodes and nanofibers are inside the PVDF film and the measurement data are normalized capacitance values, the capacitance value still shows a relative increase under pressure loading in spite of the surface contamination of the device. Therefore, peaks caused by blood pulse or breathing can be obtained.

A piece of copper tape was used to connect the AgNWs on the upper and lower PVDF films to the measurement system. Similarly, multiple wires were connected between the sensor and the measurement instrument, which may cause the overall resistance of the system to increase. However, because the sensor characterization is mainly dependent on the capacitance measurement, theoretically, the resistivity of the electrode does not affect the performance of the sensor. However, the capacitance is not a parameter that can be directly measured, the measurement must rely on an inductance−capacitance−resistance (LCR) meter. An LCR meter measures the capacitance through charging the capacitor using AC current. If the resistance of the circuit is too high or the oscillation frequency is too fast, an error may occur. In order to verify whether the capacitance result can be affected by the resistance, we have compared the output of the sensor by connecting a resistor in series with the sensor. By using an oscillation frequency of 500 kHz and a 1 kΩ resistor in series with the sensor, we simulated a poor measurement environment. The result shows that at least 500-kHz frequency and a 1-kΩ resistor give no obvious effect on the capacitance measurement. Since the AgNWs layer shows a very low sheet resistance, we believe that neither the resistance generated by wire connection nor the resistance increase caused by the spray coating process will affect the sensitivity measurement of the sensor.

Forces ranging from 0−3 N were applied to the sensor using the force application system shown in Figure S1. Considering the effective area of the contact tip, this range corresponds to pressure of up to 40 kPa. The tactile sensation of pressure corresponds to pressure ranging from a light touch to that felt when handling a heavy object.

https://dx.doi.org/10.1021/acsami.0c00448
ACS Appl. Mater. Interfaces XXXX, XXX, XXX−XXX

The sensitivity of a capacitive pressure sensor, S, is usually defined as $S = (\Delta C/C_0)/P$, where P is the applied pressure and C_0 and ΔC are the unburdened capacitance and the change in capacitance after applying a given pressure, respectively. Note that our flexible pressure sensor is a metal−insulator−metal sandwiched structure. Thus, it behaves as a conventional parallel-plate capacitor as $C = \varepsilon_r\varepsilon_0 A/d$, where d is the distance between the upper and lower electrodes, ε_0 and ε_r are the vacuum permittivity and relative permittivity of the dielectric material, respectively, and A is the overlapping area of the two electrodes.[48] When the dielectric layer is composed of a soft material, we can expect significant mechanical deformation in response to an applied load. Therefore, d is the dominant factor that converts changes in applied pressure into changes in capacitance. Compared to sensors based on solid dielectrics, nanofiber-based sensors are much more easily deformed under lower pressure, resulting in greater sensitivity.

Each of the substances in the membrane (nanofiber, bead, and air) affect the total capacitance of the device. Since all of these substances are evenly distributed inside the membrane, the device capacitance can be regarded as a series of capacitances, as follows:

$$1/C_{sq} = 1/C_{nanofiber} + 1/C_{bead} + 1/C_{air}$$

The nanofibers and beads are not elastic materials and are tightly packed against each other such that the application of an external pressure would have minimal impact on $C_{nanofiber}$ and C_{bead}. Only C_{air} strongly affects the overall device capacitance. Under pressure, air is squeezed from the film, increasing the overall C_{sq}.

Increasing the dielectric volume by introducing air gaps reduces the ability of a material to resist mechanical deformation under pressure, and increases the sensitivity of a pressure sensor.[49−51] In our system, mixing microbeads into PVDF fibers introduced air gaps into the final membrane, resulting in a more porous and compressible material.

Different electrospinning conditions were evaluated to better understand the mechanism of pressure sensing by electrospun nanofiber membranes. We first investigated the relationship between electrospinning time and sensitivity. Electrospinning time can be used to control the thickness of the dielectric layer. Relative changes in capacitance ($\Delta C/C_0$) as a function of electrospinning time and applied pressure are plotted in Figure 2a. Large $\Delta C/C_0$ differences were observed with different electrospinning times. Sensors fabricated with an electrospinning time of 20 min showed a good sensitivity of 1.12 kPa^{-1} over a range of 0−1 kPa. In contrast, sensors fabricated using a 5 min electrospinning time showed a sensitivity of 0.05 kPa^{-1} in the low pressure range. Figure 2b shows the thickness of our nanofibrous membranes (indicated by cross-sectional SEM images) made with electrospinning times of 5, 10, 20, and 60 min.

The nanofiber stack in the 5 min sample is thinner than the bead diameter. Even when no pressure is applied, the beads directly support the upper electrode, leaving little room for compression. As a result, reducing the distance between the two electrodes is difficult. Conversely, increasing the electrospinning time to 60 min results in a soft and thick nanofiber stack that is more easily compressed by an external pressure. Even a very slight pressure was sufficient to deform the nanofibrous membrane and produce a measurable change in capacitance. Thus, increasing the electrospinning time increases the thickness of the nanofiber membrane and results

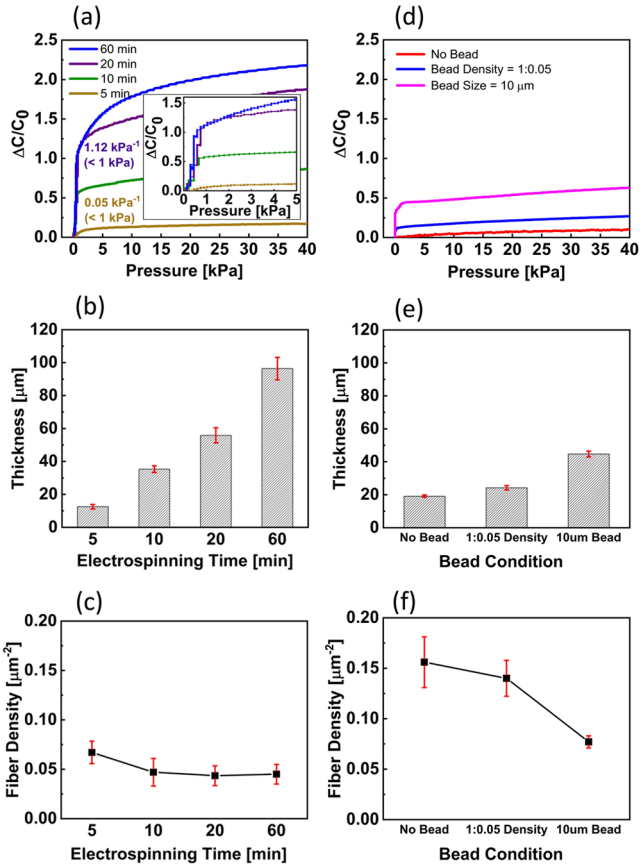

Figure 2. Influence of preparation conditions on nanofiber/microbead membranes. The influences of electrospinning time and bead conditions, respectively, are shown for (a and d) pressure-response curves, the inset shows detailed data for the 0−5 kPa region, (b and e) membrane thickness, and (c and f) membrane fiber density.

in greater sensitivity to changes in pressure. However, the relationship between electrospinning time and sensitivity is not linear. Note that the sensitivity of a 60 min sample is just slightly higher than that of a 20 min sample, not as much as the increment in preparation time. The reason may lie in the limited increment of the thickness variability.

First, the membrane thickness does not increase for a large scale while spinning process. During electrospinning, the growing nanofiber layer acts as an insulator on the collector, effectively weakening the electric field between the nozzle and the membrane surface. Newly generated nanofibers tend to be deposited more diffusely, rather than falling to the center of the collector. We have observed that longer electrospinning times result in a larger coverage area on the collector (Figure S2).

Also, the membrane shrinks during sensor fabrication. In order to minimize the gap between nanofibrous membrane and the electrodes, we have to fabricate the sensor through a lamination process. Since the lamination is carried out with external pressure on both sides of the sensor, the thickness of the sensing layer is smaller than the nanofiber which was just prepared. In this process, thick membranes are more easily affected.

Besides, Figure 2b shows that, when the electrospinning time reaches 60 min, the thickness of the membrane could be over 100 μm. However, the thickness of the PVDF substrate is less than 10 μm, which means that the nanofibrous membrane is much thicker than the substrate. So, severely wrinkled PVDF

https://dx.doi.org/10.1021/acsami.0c00448
ACS Appl. Mater. Interfaces XXXX, XXX, XXX−XXX

film was formed due to the internal stress generated by the nanofibers during drying. Therefore, a 60 min electrospinning time is not a good choice from multiple perspectives, and the excessively long preparation time contradicts the purpose of our research.

Interestingly, the overall sensitivity of the 10 min membrane is lower than that of the 20 min membrane, while exhibiting a similar sensitivity in the low-pressure region. These two membranes have the same bead density and similar porosity. Since a nanofibrous membrane is not in a bulk state, its porosity can be represented by the average distance between two adjacent fibers. This distance can be defined as the number of fibers per unit area in a cross section, i.e., fiber density. Since nanofibers can be deformed easily during slicing, we obtained accurate cross section information by embedding the membranes in PDMS resin. After the PDMS has cured, a cross section can be obtained by cutting the embedded assembly with a sharp blade. Fiber density can be calculated from SEM images of the resulting cross sections. Figure 2c shows that the highest fiber density was obtained with an electrospinning time of 5 min. This is consistent with our observations of the membrane surface, which showed only a small number of beads through the entangled nanofibers (Figure 1b). The beads and the fibers do not form an effective porous structure when the electrospinning time is short. Fiber density decreases gradually with increasing electrospinning time and remains low even after the thickness of the membrane exceeds the bead diameter. Note that the 10-, 20-, and 60 min membranes increased in thickness while maintaining a fiber density of approximately 0.045 μm^{-2}. Since all of these samples were fabricated using the same nanofiber solution, they maintained the same nanofiber-to-bead ratio, and therefore the same fiber density, regardless of the electrospinning time.

Based on the capacitance formula we have shown above, capacitance is closely related to the thickness of the nanofibrous membrane. Similar to other microstructured pressure sensors, plots of sensitivity as a function of applied pressure showed two distinct regions: a low-pressure range (0−5 kPa) and a high pressure range (5−40 kPa).

In the early stage of pressure application, fluffy nanofibers are the main factor causing great deformation. The nanofibrous membrane overall shows a low Young's modulus, so even a slight pressure will cause a severe thickness change. For this reason, the sensor shows high sensitivity in the low pressure region.

With pressure greater than 5 kPa, the capacitance of the sensor continues to change, but with much less sensitivity, as evidenced by the flattened response slope. The membrane becomes denser as pressure increases, resulting in increasing resistance to further compression and correspondingly smaller changes in capacitance for a given change in pressure. Due to the existence of the microbeads, nanofibers can still remain porous at this stage. However, the overall Young's modulus is much larger than in the early stage, leading to a decrease in sensitivity. Figure S3a shows SEM images that illustrate the behavior of the microbeads under heavy pressure. We applied heavy pressure (100 kPa) to nanofibrous membranes at 150 °C to fix the compressed membrane for observation; this temperature is slightly lower than the melting point of PVDF, allowing the nanofiber structure to remain unchanged. The microbeads in these membranes did not break and remained distributed throughout the membrane as it was compressed. These data indicate that the bead is not acting simply as a spacer but is also helping to maintain the porous structure of the membrane during compression. On the other hand, the microbeads were wrapped by nanofibers (Figure 1) and anchored to form a porous structure with multiple nanofibers, so the position of the microbeads were tightly fixed in the membrane. This stable membrane structure ensures high stability of the sensor.

Previous study has shown that PMMA could remain intact under pressures in the tens of MPa range.[52] Therefore, even if the applied pressure is higher than the test range, the bead is less likely to break (Figure S3b). If the pressure is far beyond the limit, however, the bead may lose its ability to recover to original spherical shape. The membrane will be more similar to a pure nanofibrous membrane due to the decrease of the large size spacers. As a result, the normalized capacitance change will decrease.[53]

Sensitivity curves of nanofiber membrane-based sensors without beads are shown in Figure 2d. Without the spacer effect of the beads, the membranes showed very high fiber densities, even with an electrospinning time of 20 min (Figure 2e,f) and smaller volumes of trapped air. Most notably, sensors without beads showed a poor response in the low-pressure range. Even with an electrospinning time of 60 min, the membrane without beads was incredibly dense, but with a pressure sensitivity that was still lower than that of the hybrid nanofiber membrane (Figure S4).

The effect of the nanofiber-to-microbead weight ratio on sensor performance was also evaluated. Reducing this ratio to 1:0.05 resulted in sensors with fairly low sensitivity (Figure 2d). Reducing the proportion of beads reduced membrane porosity. With an electrospinning time of 20 min, the membrane thickness was comparable to the bead diameter (Figure 2e). However, almost all of the beads were protruding from the membrane surface, indicating that the beads were not able to fully embed in the nanofibers. For the reasons discussed above, membranes made with insufficient beads performed similarly and exhibited similar fiber densities to those lacking beads entirely.

We also fabricated membranes with 10-μm beads to study the effects of bead size on sensor performance. The nanofiber-to-microbead weight ratio was maintained at 1:0.2, as with our initial sensors. Compared to porous nanofibers, microbeads are solid inside. So, there are not many microbeads distributed in the hybrid nanofibrous membrane. Due to the small quantity, the probability of microbeads stacking up on each other is very low. When the thickness of the membrane decreases under pressure, all these beads will be distributed on the same plane and share the pressure. Because the 10-μm beads are smaller in size as spacers, the variable range of membrane thickness is smaller. Halving the radius of the bead while maintaining the weight ratio theoretically increases the number of beads in a given membrane by a factor of 8. Thus, the entire membrane will be filled with a large number of small beads. Accordingly, membranes containing more beads are more capable of withstanding external pressures, so the resulting sensor showed lower sensitivity (Figure 2d). Hereafter, all experiments were performed with 20-μm beads in PVDF nanofibers at a weight ratio of 1:0.2 and an electrospinning time of 20 min.

We also studied pore size distribution to understand how electrospinning conditions affect the porosity of nanofiber membranes. In order to obtain accurate pore size distribution information, we conducted mercury intrusion porosimetry test to the samples. Because of the nonwetting property of the

https://dx.doi.org/10.1021/acsami.0c00448
ACS Appl. Mater. Interfaces XXXX, XXX, XXX−XXX

mercury, external pressures are required to force mercury enter into pores of a specific size. With this instrument, we can measure the pore distribution from 0.003 to 360 μm, which is enough for our study. The relationship between log differential intrusion and pore size diameter is shown in Figure 3; Figure 3a shows the pore size distribution as a function of electrospinning time between 5 and 60 min. Pore sizes were substantially smaller than the bead diameter, so pores larger than 20 μm can be ignored. All four samples showed a pore size distribution characterized by a broad peak between 1 and 10 μm. Furthermore, as speculated above, the 5 min sample contained a very small peak due to the absence of an effective network structure. This peak increased with electrospinning time and stabilized with electrospinning times greater than 20 min. Figure 3b shows that 20 min samples, containing either no beads, few beads, or small beads, yielded a single peak at around 1 μm, indicating low porosity. These results are consistent with our conclusions based on the fiber density calculations discussed above.

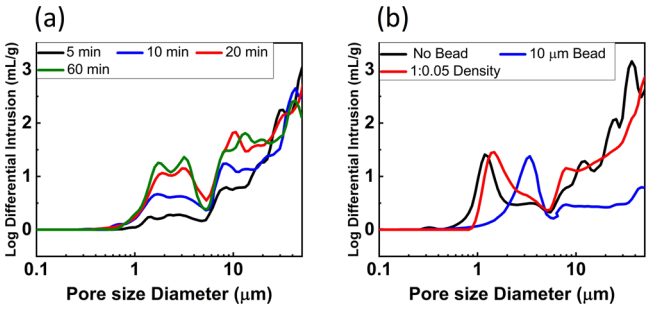

Figure 3. Pore size distributions in nanofibrous membranes are shown for (a) electrospinning times between 5 and 60 min and (b) membranes made with different bead conditions.

In order to find out whether the air gaps in the dielectric layer really play a role in pressure measurement, we used a comma roll coater to prepare a nylon film with beads that does not contain air gaps at all.[54] Figure S5a shows the surface SEM image of the film. The film did contain microbeads, and each of the beads protruded from the film surface. Such a structure ensures that the pressure can be directly applied to the microbeads during operation without being affected by the presence of air gaps. Due to the lack of the air gaps and deformable structure, a poor pressure response curve was shown (Figure S5b) when the film was applied into a pressure sensor. Therefore, we can confirm that the high pressure sensitivity shown by nanofibrous membrane is obviously due to the large air gaps caused by the composite structure.

We also investigated changes in sensor response during repeated pressure cycling. Figure 4a shows a plot of $\Delta C/C_0$ and applied force as a function of time. Capacitance increased with applied pressure, indicating that the distance between the upper and lower electrodes decreased and returned to its initial state after the pressure was removed. These data show that the PVDF nanofibers exhibit excellent recovery properties; the nanofibrous membrane fully reverts to its original thickness in the absence of an applied pressure.

A practical sensor must maintain consistent performance. Hysteresis between loading and unloading processes will affect the measurement accuracy. Hysteresis is especially noticeable in devices incorporating viscoelastic materials, often resulting in slow recovery or permanent capacitance changes. Figure 4b shows only a small amount of hysteresis over the applied pressure range, indicating that our sensors are mechanically stable and that changes in capacitance reliably indicate changes in external pressure. Figure S6 shows that $\Delta C/C_0$ as a function of pressure is consistent under different pressing speeds. This behavior was also repeatable, as evidenced by data obtained during three sequential pressure cycles of up to 1, 5, 10, 25, and 40 kPa. The data in Figure 4c show that repeatable and reliable pressure-sensing capabilities were observed from 1−40 kPa. Our sensors were able to distinguish changes in pressure even up to 40 kPa. Since typical tactile pressures are around 10 kPa, our sensors are suitable for monitoring the tactile pressures encountered during daily activities.

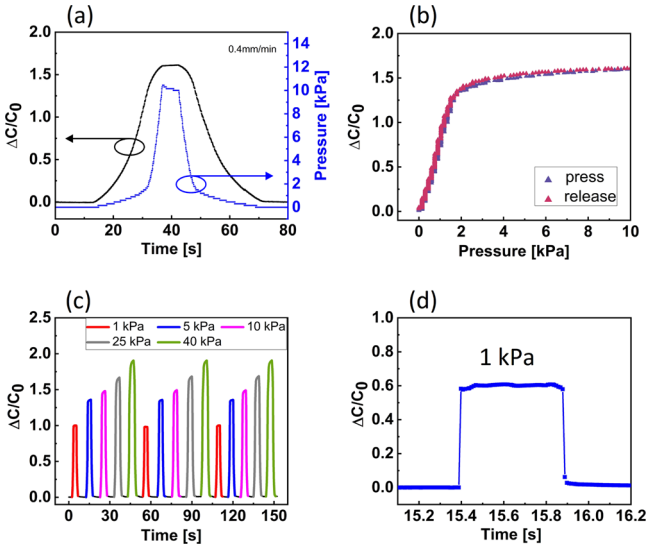

Figure 4. Sensing performance of pressure sensors employing a nanofibrous membrane dielectric. (a) Dynamic sensor response and (b) hysteresis characteristics are shown at pressures ranging from 0 to 10 kPa. (c) Sensor response is shown over triplicate sequential pressure cycles from 0 to 1, 5, 10, 25, and 40 kPa. (d) Time-resolved changes in capacitance are shown upon loading and unloading.

Another important property of practical tactile sensors is a low response lag. Figure 4d shows time-resolved capacitance changes during a loading−unloading cycle. These data are shown in detail in Figure S7. A sharp increase and decrease in capacitance were observed with loading and unloading, respectively, and both the response and relaxation times were less than 10 ms. Note that the maximum sampling rate of our LCR meter is 100 kHz. Thus, the fastest measurable sensor response is 10 ms. More accurate measurements of response and relaxation times require equipment with a higher sampling rate. However, 10 ms is still relatively fast compared with other high-sensitivity pressure sensors.[55]

Figure 5a,b demonstrates the response of a pressure sensor during more than 10 000 repeated loading−unloading cycles of 0−10 and 0−40 kPa, respectively. In both groups of experiments, the pressure holding time was 1 s. Stable responses were observed regardless of the magnitude of the applied pressure. It can therefore be inferred that the nanofibrous membranes exhibit excellent stability and durability over their full sensing range. Another important issue that can be caused by repeated pressure is the mechanical damage of the electrodes. However, due to the post annealing of the electrodes, the AgNWs is protected by the PVDF film and shows a great resistance to mechanical scratching. Figure

https://dx.doi.org/10.1021/acsami.0c00448
ACS Appl. Mater. Interfaces XXXX, XXX, XXX−XXX

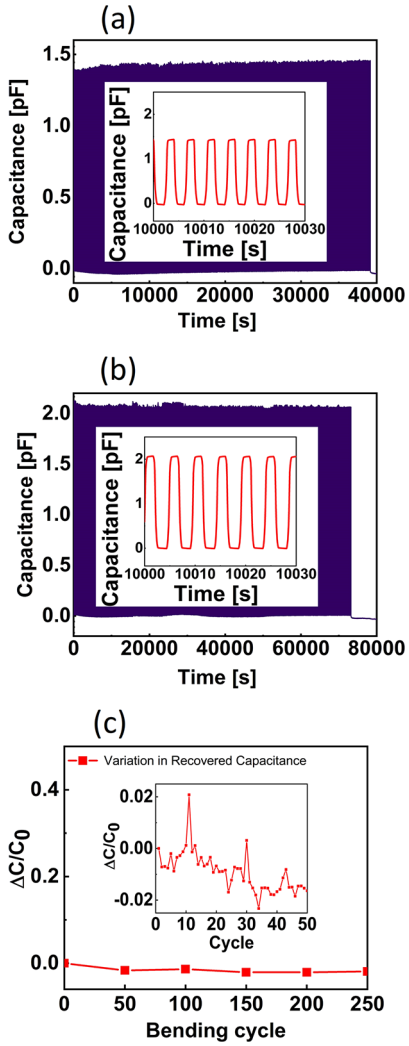

Figure 5. Long-term stability of nanofiber/microbead pressure sensors was evaluated over 10 000 cycles of an (a) 10 kPa and (b) 40 kPa pressure test. Insets show enlarged views of the testing data. (c) The variation in recovered capacitance of nanofiber/microbead pressure sensor is shown over periodic bending tests. The inset shows detailed data for the first 50 cycles.

S8 shows the surface damage of the electrode after being scratched by a cotton swab.

Compared to sensors employing rigid materials such as silicon and indium tin oxide (ITO), a pressure sensor consisting of flexible nanofibers is more suitable for use in wearable devices. This is because mechanical flexibility allows the sensor to be attached on any surface, in turn allowing a wide range of applications. To evaluate the bending stability of our flexible sensors, $\Delta C/C_0$ was measured during repeated bending and relaxing cycles. Figure 5c shows the measured capacitance as the device returns to a relaxed state after each bending cycle. Figure S9a,b shows photographs of samples being bent to radii of 13 and 27.5 mm, respectively. Notably, the capacitance deviated by only about 2% after 250 bending cycles. Being composed of a three-dimensional web-like membrane of nanofibers, the sensitivity of our sensors was not significantly affected by bending. In contrast, since the outermost layer of our sensors is a nonstretchable PVDF film, we observed that the inner electrode was wrinkled, while the outer electrode was stretched, during the bending process. This would suggest that significant changes should be observed in the capacitance of the system during bending; indeed, we did observe drastic changes in capacitance during the first 50 cycles. However, this deviation was negligible compared to the capacitance changes measured in pressure-loading experiments. To avoid this issue entirely, future sensors will employ a stretchable material, such as a thin PDMS sheet, as the electrode substrate. Overall, the capacitance of the nanofiber/bead sensors was stable during 250 bending cycles. These results can be attributed to the inherent flexibility of the nanofiber and the additional presence of strongly fixed microbeads. The thinness and stability of our sensors suggest that they may be applicable as practical wearable devices.

Flexible pressure sensors have great potential in health care applications, but their use has been limited by their thickness and weight. A device that is too bulky and/or heavy can feel awkward for the user, especially in long-term applications or during vigorous activity. Flexible, thin, and lightweight pressure sensors that must be capable of monitoring physiological processes in real-time are needed. Professional athletes, for example, are fastidious about their training and are constantly monitoring their health status. The thickness of our nanofibrous membranes is less than 60 μm and the thickness of the carrier used for the electrodes is less than 10 μm. With a total thickness of under 100 μm, ultrathin devices incorporating our sensors could be attached to any part of the body without causing abnormal sensations.

Through daily monitoring of various vital signs, some fatal diseases can be diagnosed in the early stages, thereby improving the cure rates. However, professional medical equipment is mainly located in hospitals, and medical personnel are usually scarce. Therefore, various devices to monitor health status at any time is necessary.[56] Since the human body uses breathing for metabolism all the time, monitoring the respiratory rate and volume is important for accessing the physical state of the human body. Especially, patients with asthma and pneumonia often show respiratory abnormalities, so the need for respiratory monitoring is very urgent. Moreover, because a large amount of oxygen is consumed during exercise, fatigue can be judged simply through breathing. It will be of great significance for guiding training for athletes, if the real-time monitoring of the breathing rate and intensity could be achieved. From the results above, a nanofiber based sensor shows a high sensitivity in low pressure range and is very suitable to be attached to any surface. Therefore, our sensor was integrated into a breathing mask and used to measure the respiration rate and air pressure directly. A photograph of a mask with our embedded sensor and its capacitance response during actual breathing in a relaxed state and during exercise are shown in Figure 6a,b, respectively. Since the sensor was fixed to the mask, the airflow exhaled from the mouth can be monitored directly by the sensor. The clear capacitance response indicates that our pressure sensor was highly sensitive to pressure changes caused by breathing. Each peak represents an exhalation, so we can easily measure the respiratory rate from the sensor output signals. Moreover, the respiratory intensity of each exhalation can also be estimated, since the size of each peak represents the pressure change by the airflow. Measurements acquired during exercise showed a higher capacitance response than those obtained from subjects in a relaxed state, which is consistent with reality. Considering the air volume taken at every breath is

https://dx.doi.org/10.1021/acsami.0c00448
ACS Appl. Mater. Interfaces XXXX, XXX, XXX−XXX

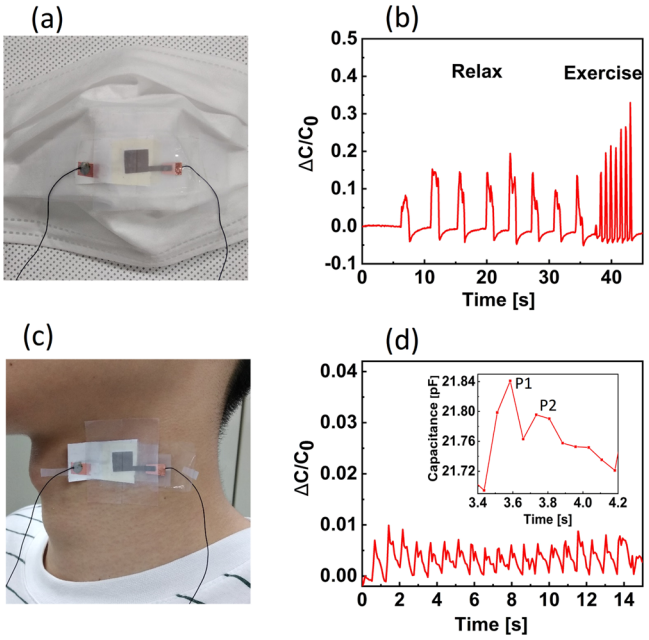

Figure 6. Various applications of nanofiber/microbead flexible pressure sensors. (a) Photograph of a face mask incorporating nanofiber/microbead pressure sensors. (b) Response curves of real-time respiratory intensity during patient relaxation and exercise. (c) Photograph of a pressure sensor directly attached to human neck skin by a commercial adhesive tape. (d) Response curves of real-time pulse detection. The inset shows a typical single pulse wave, with two peaks.

the same, an increase in frequency will lead to an increase in the air flow rate or respiratory intensity.

HR is also an important metric for tracking health, and is used for early diagnosis of multiple disorders. Most of the wearable devices are equipped with a HR monitoring module as a core feature. Our sensor was employed in a real-time carotid artery pulse monitor by attaching it directly to human neck skin using commercial adhesive tape, as shown in Figure 6c; the results are shown in Figure 6d. It should be noted that our sensor is very thin and could be attached to skin like a medical patch without bringing a strong abnormal sensation. The high sensitivity of the sensor in the low pressure region resulted in peaks corresponding to arterial pulses clearly evident over the background noise. We have concluded that the mechanism of the sensor working in the low pressure region is the membrane thickness change caused by the deformation of the fluffy nanofibers. Obviously, because the sensor is closely attached to the body, the carotid artery pressure can effectively press the nanofibers. Consistent with the actual pulse rate, the number of peaks obtained through measurement was 78 beats per minute, as would be expected for a healthy male in his 20s.[57] The fast response time and high sensitivity also allow for high-resolution pulse measurements. The inset of Figure 6d shows that two minor peaks were acquired for each pulse. Consistent with previous reports, P1 and P2 in the radial artery pressure wave indicate the systolic and diastolic peaks, respectively.[58] These results demonstrate that thin film flexible pressure sensors based on nanofiber membranes are suitable for monitoring clinical parameters and health status in real time.

We designed and fabricated a 5 × 5 array of nanofiber/microbead membrane sensors to verify multitouch recognition. Figure 7a,b shows schematics of the sensor array. Five AgNW

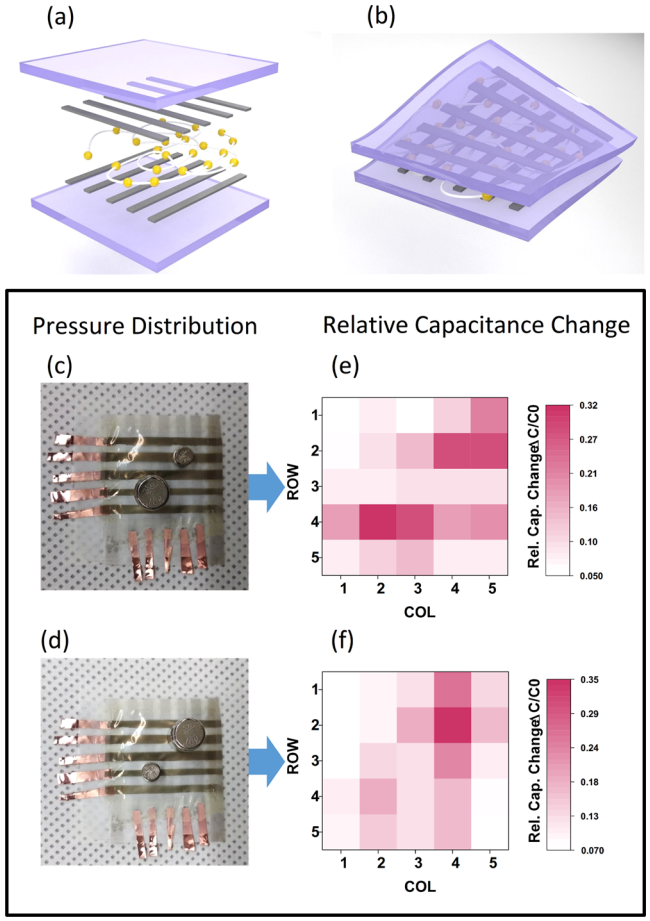

Figure 7. Schematic illustration of an array of nanofiber/microbead flexible pressure sensors. (a) Schematic diagram of the capacitive sensor array. (b) Schematic diagram of a flexible capacitive pressure sensor array. Panels c and d show photographs of two weights (1 and 10 g, respectively) on the sensor array. Panels e and f show pressure distribution maps created based on the output of the sensor array.

electrodes were sprayed in parallel through a screen mask onto both the upper and lower substrates. Each AgNW electrode was a 3 mm-wide stripe. The electrodes on the upper and lower substrates were then positioned orthogonally and face-to-face with a layer of pressure-sensitive membrane between them. In this way, each crossing point of the electrodes was a sensor cell, or pixel, with the total array consisting of 25 pixels. Sensor maps were created by building a signal collection system and connecting the prepared sensor array, as shown in Figure S10. A microcontroller unit (MCU) was used to address each sensor cell so that capacitance signals from the entire array could be scanned and recorded in sequence. Figure 7c,d shows photographs of 1- and 10-g weights on a sensor array, respectively. Pressure distribution maps, generated from the combined sensor pixel data, are shown in Figure 7e,f. The pressure distribution maps were consistent with the applied weights, even when the positions of the two weights were switched. In addition, the bottom area of the 10-g weight is larger than the sensing area of a single sensor pixel, such that a proportional increase was observed in the capacitance of neighboring pixels. Additional crosstalk between pixels indicates a lack of efficient pixel separation. Bonding methods, such as ultrasonic bonding, could be used to isolate individual pixels between the electrodes and the nanofibers. These results

https://dx.doi.org/10.1021/acsami.0c00448
ACS Appl. Mater. Interfaces XXXX, XXX, XXX−XXX

Table 2. Comparison with the State-of-the-Art PVDF-Based Sensors

material	form	sensor type	sensitivity	static pressure detection	pressure range	ref
PVDF-TrFE/rGO/MCNTs/PEDOT	nanofiber	piezoelectric	67.4/kPa	no	5−30 kPa	59
PVDF/GO	nanofiber	piezoelectric	4.3 V/kPa	no		60
PVDF	foil	piezoelectric	3.6 mV/Pa	no		61
PVDF	nanofiber	piezoelectric	0.02 V/kPa	no	30−110 kPa	62
PVDF/CNT	nanofiber	piezoelectric	2.26 mV/N	no	200−350 N	63
PVDF/PMMA	nanofiber	capacitive	1.12/kPa	yes	0−40 kPa	this work

show that each sensor pixel was able to independently respond to an applied pressure; this behavior allows pressure distribution to be mapped on a sensor array. The development of a sensor array consisting of nanofiber/microbead pressure sensors significantly reduces the gap between such high-performance materials and practical applications.

3. CONCLUSIONS

This study demonstrates flexible, durable, and highly sensitive capacitive pressure sensors based on electrospun PVDF nanofibers incorporating insulating polymer microbeads. A polymer solution containing PVDF nanofibers and microbeads was electrospun and fabricated into an ultrathin membrane. The microbeads were uniformly distributed throughout the nanofiber membrane and acted as dielectric spacers. The presence of the microbeads resulted in highly deformable and sensitive sensors, even at very low pressures. By using different electrospinning parameters to prepare nanofibrous membranes, we found that controlling the concentration of microbeads in the PVDF nanofiber solution and electrospinning time significantly affect the air gaps in the nanofiber membrane, and further tailor the sensitivity of the sensor.

Our pressure sensor exhibited a sensitivity of up to 1.12 kPa^{-1} over a range of 0−1 kPa and a wide dynamic range of up to 40 kPa without any significant loss in sensitivity. The PVDF nanofiber was fluffy and showed good recovery after compression, resulting in low hysteresis and fast response-relaxation times of less than 10 ms. The sensors were also stable over 10 000 loading−unloading cycles and 250 bending cycles up to a radius of 13 mm.

Compared with materials with high elasticity such as PDMS or Ecoflex, PVDF has no significant advantages in terms of resilience and deformability. Therefore, rather than capacitive sensors, PVDF has been focused on fabricating into piezoelectric sensors (Table 2), because of the high piezoelectric coefficient. Usually, these sensors show advantages such as self-power, high signal-to-noise ratio, and good linearity. However, the measurable pressure range is usually very high, and large errors were shown during static pressure measurement.

Meanwhile, in this article, our sensor showed high availability in low pressure range and no obvious error under static pressures. The main disadvantages are poor resistance to electromagnetic interference and poor linearity. These are mainly due to the different sensing mechanisms of the sensors. Besides, due to the different signal types (capacitance, voltage, and current) and evaluation standards, it is relatively difficult to directly compare the sensitivity among the sensors with different sensing mechanisms.

Thus, our nanofiber-based pressure sensors solved the technical challenges of easy fabrication and high performance while having the additional advantages of being lightweight and thin, thus exhibiting potential for applications in wearable devices. To show the utility of our pressure sensors as a wearable healthcare device, we demonstrated respiratory rate and HR monitoring applications. Finally, a 5 × 5 sensor array was fabricated and used to measure the spatial distribution of applied pressures. We believe that our pressure sensors based on electrospun PVDF nanofibers incorporating insulating polymer microbeads will be useful in the development of flexible, durable, and highly sensitive applications such as tactile sensors, electronic skin, and wearable health monitoring sensors.

4. EXPERIMENTAL SECTION

4.1. Device Fabrication. Commercially available PVDF powder (Solvay) was dissolved in acetone and butanone cosolvent and sonicated for 24 h to form a uniformly distributed 20 wt % PVDF solution. A 10-μm-thick PVDF film was cast onto a glass slide using a film applicator and thermally dried at 50 °C for 10 min. Conducting AgNWs (Nanopyxis Co., Ltd.) were spray-coated on the PVDF films, and the coating process was repeated several times to reduce electrical resistivity. A 1 cm × 1 cm electrode pattern was made by applying a prepatterned screening mask while spray coating. Then the AgNWs/PVDF film was annealed at 140 °C on a hot plate to remove the inner stress. At the same time, as the melted PVDF can penetrate into the AgNWs microweb structure, this postannealing process also increases the mechanical stability of the electrode. Peeling the dried film off of the glass slide yielded AgNW-coated PVDF films.

PVDF powder was also dissolved in dimethylacetamide and acetone to form a 20 wt % nanofiber solution. A calculated weight of insulating PMMA beads (S20; Duksan Hi-Metal Co., Ltd.) was then mixed into the nanofiber solution prior to electrospinning. This mixed solution was stirred vigorously to obtain a homogeneous distribution of microbeads. In the next step, electrospinning was used to fabricate nanofibrous membranes incorporating the insulating microbeads. For electrospinning, the working distance between the syringe nozzle and the collector was 10 cm. A 10 kV voltage was applied between the syringe and the collector. During the electrospinning process, the AgNWs/PVDF film was placed on the collector such that the nanofibrous membrane was deposited directly on the AgNW electrode. Finally, a laminate structure consisting of two patterned AgNWs/PVDF electrodes and a nanofibrous/microbead membrane was used as an array of pressure sensors to measure pressure distribution on a surface.

4.2. Characterization and Measurements. Membrane thickness and the distribution of microbeads were characterized by SEM (Nova NanoSEM 230; FEI). Pore size distribution data was obtained from a Mercury Porosimeters (Auto Pore IV; micromeritics). A custom measurement system was built to measure the mechanical-capacitance response of the pressure sensors. A digital force gauge (M5-2; Mark-10) with a plastic tip was installed on a motorized test stand (ESM 303; Mark-10) to apply programmed pressures to the sensor. The fabricated pressure sensor was fixed on a sample stage and connected to an LCR meter (E4980A; Agilent). The capacitance was measured at a frequency of 500 kHz with 1-V bias voltage. During pressure testing, a plastic tip was used to apply pressure to the sample with the digital force gauge. The plastic tip was square with a side length of 8 mm. The sensor output and the real-time force values were recorded simultaneously with a PC.

https://dx.doi.org/10.1021/acsami.0c00448
ACS Appl. Mater. Interfaces XXXX, XXX, XXX−XXX

■ ASSOCIATED CONTENT

Supporting Information

The Supporting Information is available free of charge at https://pubs.acs.org/doi/10.1021/acsami.0c00448.

Measurement setup; membrane coverage areas; membrane surface morphology during pressure testing; pressure-response curves for pressure sensors composed of membranes without microbeads; pressure sensor composed of nylon films and microbeads; hysteresis of nanofiber/microbead pressure sensors; response and relaxation times; surface damage of the electrodes after being scratched by a cotton swab; bending tests; and sensor array signal collection system (PDF)

Real-time monitoring of respiratory intensity (MP4)

Real-time pulse monitoring (MP4)

■ AUTHOR INFORMATION

Corresponding Author

Sang-Hee Ko Park − *Department of Materials Science and Engineering, Korea Advanced Institute of Science and Technology (KAIST), Daejeon 305-701, South Korea;* orcid.org/0000-0001-7165-8211; Email: shkp@kaist.ac.kr

Authors

Taiyu Jin − *Department of Materials Science and Engineering, Korea Advanced Institute of Science and Technology (KAIST), Daejeon 305-701, South Korea;* orcid.org/0000-0002-0315-8650

Yan Pan − *Department of Materials Science and Engineering, Korea Advanced Institute of Science and Technology (KAIST), Daejeon 305-701, South Korea*

Guk-Jin Jeon − *Department of Materials Science and Engineering, Korea Advanced Institute of Science and Technology (KAIST), Daejeon 305-701, South Korea*

Hye-In Yeom − *Department of Materials Science and Engineering, Korea Advanced Institute of Science and Technology (KAIST), Daejeon 305-701, South Korea;* orcid.org/0000-0002-9370-2620

Shuye Zhang − *State Key Laboratory of Advanced Welding and Jointing, Harbin Institute of Technology, Harbin 150001, China;* orcid.org/0000-0003-0170-3835

Kyung-Wook Paik − *Department of Materials Science and Engineering, Korea Advanced Institute of Science and Technology (KAIST), Daejeon 305-701, South Korea*

Complete contact information is available at: https://pubs.acs.org/10.1021/acsami.0c00448

Notes

The authors declare no competing financial interest.

■ ACKNOWLEDGMENTS

This research was supported by Nano Material Technology Development Program through the National Research Foundation of Korea(NRF) funded by the Ministry of Science, ICT and Future Planning (2016M3A7B4905609).

■ REFERENCES

(1) Tee, B. C. K.; Wang, C.; Allen, R.; Bao, Z. N. An Electrically and Mechanically Self-healing Composite with Pressure- and Flexion-sensitive Properties for Electronic Skin Applications. *Nat. Nanotechnol.* **2012**, *7*, 825−832.

(2) Yetisen, A. K.; Qu, H.; Manbachi, A.; Butt, H.; Dokmeci, M. R.; Hinestroza, J. P.; Skorobogatiy, M.; Khademhosseini, A.; Yun, S. H. Nanotechnology in Textiles. *ACS Nano* **2016**, *10*, 3042−3068.

(3) Li, L. H.; Bai, Y. Y.; Li, L. L.; Wang, S. Q.; Zhang, T. A Superhydrophobic Smart Coating for Flexible and Wearable Sensing Electronics. *Adv. Mater.* **2017**, *29*, 1702517.

(4) Eom, J.; Heo, J. S.; Kim, M.; Lee, J. H.; Park, S. K.; Kim, Y. H. Highly Sensitive Textile-Based Strain Sensors Using Poly(3,4-ethylenedioxythiophene):PolystyreneSulfonate/Silver Nanowire-Coated Nylon Threads with Poly-l-lysine Surface Modification. *RSC Adv.* **2017**, *7*, 53373−53378.

(5) Heo, J. S.; Eom, J.; Kim, Y. H.; Park, S. K. Recent Progress of Textile-Based Wearable Electronics: A Comprehensive Review of Materials, Devices, and Applications. *Small* **2018**, *14*, 1703034.

(6) Sinha, T. K.; Ghosh, S. K.; Maiti, R.; Jana, S.; Adhikari, B.; Mandal, D.; Ray, S. K. Graphene-Silver-Induced Self-Polarized PVDF-Based Flexible Plasmonic Nanogenerator Toward the Realization for New Class of Self Powered Optical Sensor. *ACS Appl. Mater. Interfaces* **2016**, *8*, 14986−14993.

(7) Gao, N. W.; Zhang, X. Y.; Liao, S. L.; Jia, H. Y.; Wang, Y. P. Polymer Swelling Induced Conductive Wrinkles for an Ultrasensitive Pressure Sensor. *ACS Macro Lett.* **2016**, *5*, 823−827.

(8) Lee, C. J.; Park, K. H.; Han, C. J.; Oh, M. S.; You, B.; Kim, Y. S.; Kim, J. W. Crack-Induced Ag Nanowire Networks for Transparent, Stretchable, and Highly Sensitive Strain Sensors. *Sci. Rep.* **2017**, *7*, 7956.

(9) Tai, Y. L.; Yang, Z. G. Flexible Pressure Sensing Film Based on Ultrasensitive SWCNT/PDMS Spheres for Monitoring Human Pulse Signals. *J. Mater. Chem. B* **2015**, *3*, 5436−5441.

(10) Parida, K.; Bhavanasi, V.; Kumar, V.; Bendi, R.; Lee, P. S. Self-Powered Pressure Sensor for Ultra-Wide Range Pressure Detection. *Nano Res.* **2017**, *10*, 3557−3570.

(11) Doshi, S. M.; Thostenson, E. T. Thin and Flexible Carbon Nanotube-Based Pressure Sensors with Ultrawide Sensing Range. *ACS Sens.* **2018**, *3*, 1276−1282.

(12) Yue, Y.; Liu, N. S.; Liu, W. J.; Li, M. A.; Ma, Y. A.; Luo, C.; Wang, S. L.; Rao, J. Y.; Hu, X. K.; Su, J.; Zhang, Z.; Huang, Q.; Gao, Y. H. 3D Hybrid Porous Mxene-Sponge Network and Its Application in Piezoresistive Sensor. *Nano Energy* **2018**, *50*, 79−87.

(13) Luo, C.; Liu, N. S.; Zhang, H.; Liu, W. J.; Yue, Y.; Wang, S. L.; Rao, J. Y.; Yang, C. X.; Su, J.; Jiang, X. L.; Gao, Y. H. A New Approach for Ultrahigh-Performance Piezoresistive Sensor Based on Wrinkled PPy Film with Electrospun PVA Nanowires as Spacer. *Nano Energy* **2017**, *41*, 527−534.

(14) Li, H. X.; Liu, N. S.; Zhang, X. H.; Su, J.; Li, L. Y.; Gao, Y. H.; Wang, Z. L. Piezotronic and Piezo-Phototronic Logic Computations Using Au Decorated ZnO Microwires. *Nano Energy* **2016**, *27*, 587−594.

(15) Liu, W. J.; Liu, N. S.; Yue, Y.; Rao, J. Y.; Cheng, F.; Su, J.; Liu, Z. T.; Gao, Y. H. Piezoresistive Pressure Sensor Based on Synergistical Innerconnect Polyvinyl Alcohol Nanowires/Wrinkled Graphene Film. *Small* **2018**, *14*, 1704149.

(16) Liu, W. J.; Liu, N. S.; Yue, Y.; Rao, J. Y.; Luo, C.; Zhang, H.; Yang, C. X.; Su, J.; Liu, Z. T.; Gao, Y. H. A Flexible and Highly Sensitive Pressure Sensor Based on Elastic Carbon Foam. *J. Mater. Chem. C* **2018**, *6*, 1451−1458.

(17) Zhang, H.; Liu, N. S.; Shi, Y. L.; Liu, W. J.; Yue, Y.; Wang, S. L.; Ma, Y. N.; Wen, L.; Li, L. Y.; Long, F.; Zou, Z. G.; Gao, Y. H. Piezoresistive Sensor with High Elasticity Based on 3D Hybrid Network of Sponge@CNTs@Ag NPs. *ACS Appl. Mater. Interfaces* **2016**, *8*, 22374−22381.

(18) Mannsfeld, S. C. B.; Tee, B. C. K.; Stoltenberg, R. M.; Chen, C. V. H. H.; Barman, S.; Muir, B. V. O.; Sokolov, A. N.; Reese, C.; Bao, Z. N. Highly Sensitive Flexible Pressure Sensors with Microstructured Rubber Dielectric Layers. *Nat. Mater.* **2010**, *9*, 859−864.

(19) Boutry, C. M.; Nguyen, A.; Lawal, Q. O.; Chortos, A.; Rondeau-Gagne, S.; Bao, Z. N. A Sensitive and Biodegradable Pressure Sensor Array for Cardiovascular Monitoring. *Adv. Mater.* **2015**, *27*, 6954−6961.

https://dx.doi.org/10.1021/acsami.0c00448
ACS Appl. Mater. Interfaces XXXX, XXX, XXX−XXX

(20) Pang, C.; Koo, J. H.; Nguyen, A.; Caves, J. M.; Kim, M. G.; Chortos, A.; Kim, K.; Wang, P. J.; Tok, J. B. H.; Bao, Z. A. Highly Skin-Conformal Microhairy Sensor for Pulse Signal Amplification. *Adv. Mater.* **2015**, *27*, 634−640.
(21) Tee, B. C. K.; Chortos, A.; Dunn, R. R.; Schwartz, G.; Eason, E.; Bao, Z. A. Tunable Flexible Pressure Sensors using Microstructured Elastomer Geometries for Intuitive Electronics. *Adv. Funct. Mater.* **2014**, *24*, 5427−5434.
(22) Kim, S. Y.; Park, S.; Park, H. W.; Park, D. H.; Jeong, Y.; Kim, D. H. Highly Sensitive and Multimodal All-Carbon Skin Sensors Capable of Simultaneously Detecting Tactile and Biological Stimuli. *Adv. Mater.* **2015**, *27*, 4178−4185.
(23) Kwon, D.; Lee, T. I.; Shim, J.; Ryu, S.; Kim, M. S.; Kim, S.; Kim, T. S.; Park, I. Highly Sensitive, Flexible, and Wearable Pressure Sensor Based on a Giant Piezocapacitive Effect of Three-Dimensional Microporous Elastomeric Dielectric Layer. *ACS Appl. Mater. Interfaces* **2016**, *8*, 16922−16931.
(24) Parameswaran, C.; Gupta, D. Low Cost Sponge Based Piezocapacitive Sensors Using a Single Step Leavening Agent Mediated Autolysis Process. *J. Mater. Chem. C* **2018**, *6*, 5473−5481.
(25) Pyo, S.; Choi, J.; Kim, J. Flexible, Transparent, Sensitive, and Crosstalk-Free Capacitive Tactile Sensor Array Based on Graphene Electrodes and Air Dielectric. *Adv. Electron. Mater.* **2018**, *4*, 1700427.
(26) Wang, L. X.; Peng, H. L.; Wang, X. L.; Chen, X.; Yang, C. S.; Yang, B.; Liu, J. Q. PDMS/MWCNT-Based Tactile Sensor Array with Coplanar Electrodes for Crosstalk Suppression. *Microsyst. Nanoeng.* **2016**, *2*, 1−8.
(27) Li, X.; Huang, W.; Yao, G.; Gao, M.; Wei, X. B.; Liu, Z. W.; Zhang, H.; Gong, T. X.; Yu, B. Highly Sensitive Flexible Tactile Sensors Based on Microstructured Multiwall Carbon Nanotube Arrays. *Scr. Mater.* **2017**, *129*, 61−64.
(28) Shi, M. Y.; Zhang, J. X.; Chen, H. T.; Han, M. D.; Shankaregowda, S. A.; Su, Z. M.; Meng, B.; Cheng, X. L.; Zhang, H. X. Self-Powered Analogue Smart Skin. *ACS Nano* **2016**, *10*, 4083−4091.
(29) Joo, Y.; Byun, J.; Seong, N.; Ha, J.; Kim, H.; Kim, S.; Kim, T.; Im, H.; Kim, D.; Hong, Y. Silver Nanowire-Embedded PDMS with a Multiscale Structure for a Highly Sensitive and Robust Flexible Pressure Sensor. *Nanoscale* **2015**, *7*, 6208−6215.
(30) Park, S.; Kim, H.; Vosgueritchian, M.; Cheon, S.; Kim, H.; Koo, J. H.; Kim, T. R.; Lee, S.; Schwartz, G.; Chang, H.; Bao, Z. A. Stretchable Energy-Harvesting Tactile Electronic Skin Capable of Differentiating Multiple Mechanical Stimuli Modes. *Adv. Mater.* **2014**, *26*, 7324−7332.
(31) Luo, Y. S.; Shao, J. Y.; Chen, S. R.; Chen, X. L.; Tian, H. M.; Li, X. M.; Wang, L.; Wang, D. R.; Lu, B. H. Flexible Capacitive Pressure Sensor Enhanced by Tilted Micropillar Arrays. *ACS Appl. Mater. Interfaces* **2019**, *11*, 17796−17803.
(32) Wang, X. W.; Gu, Y.; Xiong, Z. P.; Cui, Z.; Zhang, T. Silk-Molded Flexible, Ultrasensitive, and Highly Stable Electronic Skin for Monitoring Human Physiological Signals. *Adv. Mater.* **2014**, *26*, 1336−1342.
(33) Li, T.; Luo, H.; Qin, L.; Wang, X. W.; Xiong, Z. P.; Ding, H. Y.; Gu, Y.; Liu, Z.; Zhang, T. Flexible Capacitive Tactile Sensor Based on Micropatterned Dielectric Layer. *Small* **2016**, *12*, 5042−5048.
(34) Jian, M. Q.; Xia, K. L.; Wang, Q.; Yin, Z.; Wang, H. M.; Wang, C. Y.; Xie, H. H.; Zhang, M. C.; Zhang, Y. Y. Flexible and Highly Sensitive Pressure Sensors Based on Bionic Hierarchical Structures. *Adv. Funct. Mater.* **2017**, *27*, 1606066.
(35) Lipomi, D. J.; Vosgueritchian, M.; Tee, B. C. K.; Hellstrom, S. L.; Lee, J. A.; Fox, C. H.; Bao, Z. N. Skin-Like Sensors of Pressure and Strain Enabled by Transparent, Elastic Films of Carbon Nanotubes. *Nat. Nanotechnol.* **2011**, *6*, 788−792.
(36) Lai, Y. C.; Deng, J.; Liu, R.; Hsiao, Y. C.; Zhang, S. L.; Peng, W.; Wu, H. M.; Wang, X.; Wang, Z. L. Actively Perceiving and Responsive Soft Robots Enabled by Self-Powered, Highly Extensible, and Highly Sensitive Triboelectric Proximity- and Pressure-Sensing Skins. *Adv. Mater.* **2018**, *30*, 1801114.
(37) Lin, M. F.; Xiong, J. Q.; Wang, J. X.; Parida, K.; Lee, P. S. Core-Shell Nanofiber Mats for Tactile Pressure Sensor and Nanogenerator Applications. *Nano Energy* **2018**, *44*, 248−255.
(38) Choi, S. S.; Lee, Y. S.; Joo, C. W.; Lee, S. G.; Park, J. K.; Han, K. S. Electrospun PVDF Nanofiber Web as Polymer Electrolyte or Separator. *Electrochim. Acta* **2004**, *50*, 339−343.
(39) Park, S. H.; Lee, H. B.; Yeon, S. M.; Park, J.; Lee, N. K. Flexible and Stretchable Piezoelectric Sensor with Thickness-Tunable Configuration of Electrospun Nanofiber Mat and Elastomeric Substrates. *ACS Appl. Mater. Interfaces* **2016**, *8*, 24773−24781.
(40) Persano, L.; Dagdeviren, C.; Su, Y. W.; Zhang, Y. H.; Girardo, S.; Pisignano, D.; Huang, Y. G.; Rogers, J. A. High Performance Piezoelectric Devices Based on Aligned Arrays of Nanofibers of Poly(vinylidenefluoride-co-trifluoroethylene). *Nat. Commun.* **2013**, *4*, 1633.
(41) Zhou, Y. M.; He, J. X.; Wang, H. B.; Qi, K.; Nan, N.; You, X. L.; Shao, W. L.; Wang, L. D.; Ding, B.; Cui, S. Z. Highly Sensitive, Self-powered and Wearable Electronic Skin Based on Pressure-Sensitive Nanofiber Woven Fabric Sensor. *Sci. Rep.* **2017**, *7*, 12949.
(42) Yang, W.; Li, N. W.; Zhao, S. Y.; Yuan, Z. Q.; Wang, J. N.; Du, X. Y.; Wang, B.; Cao, R.; Li, X. Y.; Xu, W. H.; Wang, Z. L.; Li, C. J. A Breathable and Screen-Printed Pressure Sensor Based on Nanofiber Membranes for Electronic Skins. *Adv. Mater. Technol.* **2018**, *3*, 1700241.
(43) Lee, S. H.; Kim, T. W.; Suk, K. L.; Paik, K. W. Nanofiber Anisotropic Conductive Films (ACF) for Ultra-Fine-Pitch Chip-on-Glass (COG) Interconnections. *J. Electron. Mater.* **2015**, *44*, 4628−4636.
(44) Kim, Y.; Jang, S.; Kang, B. J.; Oh, J. H. Fabrication of Highly Sensitive Capacitive Pressure Sensors with Electrospun Polymer Nanofibers. *Appl. Phys. Lett.* **2017**, *111*, 073502.
(45) Cho, D.; Naydich, A.; Frey, M. W.; Joo, Y. L. Further Improvement of Air Filtration Efficiency of Cellulose Filters Coated with Nanofibers via Inclusion of Electrostatically Active Nanoparticles. *Polymer* **2013**, *54*, 2364−2372.
(46) Wan, H. G.; Wang, N.; Yang, J. M.; Si, Y. R. S.; Chen, K.; Ding, B.; Sun, G.; El-Newehy, M.; Al-Deyab, S. S.; Yu, J. Y. Hierarchically Structured Polysulfone/Titania Fibrous Membranes with Enhanced Air Filtration Performance. *J. Colloid Interface Sci.* **2014**, *417*, 18−26.
(47) Veeralingam, S.; Sahatiya, P.; Badhulika, S. Low Cost, Flexible and Disposable $SnSe_2$ Based Photoresponsive Ammonia Sensor for Detection of Ammonia in Urine Samples. *Sens. Actuators, B* **2019**, *297*, 126725.
(48) Zang, Y. P.; Zhang, F. J.; Di, C. A.; Zhu, D. B. Advances of Flexible Pressure Sensors Toward Artificial Intelligence and Health Care Applications. *Mater. Horiz.* **2015**, *2*, 140−156.
(49) Choi, W.; Choi, K.; Yu, C. Ultrafast Nanoscale Polymer Coating on Porous 3D Structures Using Microwave Irradiation. *Adv. Funct. Mater.* **2018**, *28*, 1704877.
(50) Oh, J.; Yang, J. C.; Kim, J. O.; Park, H.; Kwon, S. Y.; Lee, S.; Sim, J. Y.; Oh, H. W.; Kim, J.; Park, S. Pressure Insensitive Strain Sensor with Facile Solution-Based Process for Tactile Sensing Applications. *ACS Nano* **2018**, *12*, 7546−7553.
(51) Wu, S.; Zhang, J.; Ladani, R. B.; Ravindran, A. R.; Mouritz, A. P.; Kinloch, A. J.; Wang, C. H. Novel Electrically Conductive Porous PDMS/Carbon Nanofiber Composites for Deformable Strain Sensors and Conductors. *ACS Appl. Mater. Interfaces* **2017**, *9*, 14207−14215.
(52) Zhang, J. J.; Jin, T.; Wang, Z. H.; Zhao, L. M. Experimental Investigation on Yield Behavior of PMMA under Combined Shear-Compression Loading. *Results Phys.* **2016**, *6*, 265−269.
(53) Veeralingam, S.; Sahatiya, P.; Kadu, A.; Mattela, V.; Badhulika, S. Direct, One-Step Growth of $NiSe_2$ on Cellulose Paper: A Low-Cost, Flexible, and Wearable with Smartphone Enabled Multifunctional Sensing Platform for Customized Noninvasive Personal Healthcare Monitoring. *ACS Appl. Electron. Mater.* **2019**, *1*, 558−568.
(54) Yoon, D. J.; Lee, S. H.; Paik, K. W. Effects of the Nylon Anchoring Polymer Layer on the Conductive Particle Movements of Anisotropic Conductive Films for Ultrafine Pitch Chip-on-Glass

https://dx.doi.org/10.1021/acsami.0c00448
ACS Appl. Mater. Interfaces XXXX, XXX, XXX−XXX

Applications. *IEEE Trans. Compon., Packag., Manuf. Technol.* **2018**, *8*, 1723−1728.
(55) Wang, Z. H.; Si, Y.; Zhao, C. Y.; Yu, D.; Wang, W.; Sun, G. Flexible and Washable Poly(Ionic Liquid) Nanofibrous Membrane with Moisture Proof Pressure Sensing for Real-Life Wearable Electronics. *ACS Appl. Mater. Interfaces* **2019**, *11*, 27200−27209.
(56) Shinde, A.; Sahatiya, P.; Kadu, A.; Badhulika, S. Wireless Smartphone-Assisted Personal Healthcare Monitoring System Using a MoS_2-Based Flexible, Wearable and Ultra-Low-Cost Functional Sensor. *Flexible Printed Electron.* **2019**, *4*, 025003.
(57) Dagdeviren, C.; Su, Y. W.; Joe, P.; Yona, R.; Liu, Y. H.; Kim, Y. S.; Huang, Y. A.; Damadoran, A. R.; Xia, J.; Martin, L. W.; Huang, Y. G.; Rogers, J. A. Conformable Amplified Lead Zirconate Titanate Sensors with Enhanced Piezoelectric Response for Cutaneous Pressure Monitoring. *Nat. Commun.* **2014**, *5*, 4496.
(58) Chepuri, M.; Sahatiya, P.; Badhulika, S. Monitoring of Physiological Body Signals and Human Activity Based on Ultra-Sensitive Tactile Sensor and Artificial Electronic Skin by Direct Growth of $ZnSnO_3$ on Silica Cloth. *Mater. Sci. Semicond. Process.* **2019**, *99*, 125−133.
(59) Ahmed, A.; Jia, Y. M.; Huang, Y.; Khoso, N. A.; Deb, H.; Fan, Q. G.; Shao, J. Z. Preparation of PVDF-TrFE Based Electrospun Nanofibers Decorated with PEDOT-CNT/rGO Composites for Piezo-Electric Pressure Sensor. *J. Mater. Sci.: Mater. Electron.* **2019**, *30*, 14007−14021.
(60) Roy, K.; Ghosh, S. K.; Sultana, A.; Garain, S.; Xie, M. Y.; Bowen, C. R.; Henkel, K.; Schmeisser, D.; Mandal, D. A Self-Powered Wearable Pressure Sensor and Pyroelectric Breathing Sensor Based on GO Interfaced PVDF Nanofibers. *ACS Appl. Nano Mater.* **2019**, *2*, 2013−2025.
(61) Bobinger, M.; Keddis, S.; Hinterleuthner, S.; Becherer, M.; Kluge, F.; Schwesinger, N.; Salmeron, J. E.; Lugli, P.; Rivadeneyra, A. Light and Pressure Sensors Based on PVDF With Sprayed and Transparent Electrodes for Self-Powered Wireless Sensor Nodes. *IEEE Sens. J.* **2019**, *19*, 1114−1126.
(62) Wang, G.; Liu, T.; Sun, X. C.; Li, P.; Xu, Y. S.; Hua, J. G.; Yu, Y. H.; Li, S. X.; Dai, Y. Z.; Song, X. Y.; Lv, C.; Xia, H. Flexible Pressure Sensor Based on PVDF Nanofiber. *Sens. Actuators, A* **2018**, *280*, 319−325.
(63) Wu, C. M.; Chou, M. H.; Zeng, W. Y. Piezoelectric Response of Aligned Electrospun Polyvinylidene Fluoride/Carbon Nanotube Nanofibrous Membranes. *Nanomaterials* **2018**, *8*, 420.

https://dx.doi.org/10.1021/acsami.0c00448
ACS Appl. Mater. Interfaces XXXX, XXX, XXX−XXX